ELSEVIER

International Journal of Mass Spectrometry 214 (2002) 383–395

International Journal of Mass Spectrometry

www.elsevier.com/locate/ijms

$Ga_{19}(C(SiMe_3)_3)_6^-$ as a precursor for pure and silicon-doped gallium clusters: a mass spectrometric study of a Ga_{13}^- and a $Ga_{12}Si^-$ anion

Katharina Weiß, Ralf Köppe, Hansgeorg Schnöckel*

Institut für Anorganische Chemie, Lehrstuhl für Analytische Chemie, Engesserstr. 15, 76131 Karlsruhe, Germany

Received 3 December 2001; accepted 16 January 2002

Abstract

The metalloid cluster $[Ga_{19}(C(SiMe_3)_3)_6][Li_2Br(THF)_6]$ was studied by Fourier-transform ion cyclotron resonance-mass spectrometry (FT/ICR-MS). The spectrum obtained by laser desorption ionization (LDI) is dominated by pure gallium cluster anions Ga_n^- with n ranging up to 50 and mixed gallium–silicon cluster anions Ga_nSi^-, $Ga_nSi_2^-$, and $Ga_nSi_3^-$ with n ranging up to 43. A maximum of the cluster abundance is observed for Ga_{13}^- and $Ga_{12}Si^-$. These experimental results exhibit for the first time the formation of large pure and silicon-doped gallium clusters starting from a molecular compound. They are discussed in terms of the precursor's structure and the simplified predictions of the jellium model. DFT calculations were employed to further evaluate the electronic properties of these anionic clusters, the results of which show that Ga_{13}^- favors a regular bicapped pentagonal prism (D_{5h}) as well as $Ga_{12}Si^-$, Si being located in the center of the cluster. (Int J Mass Spectrom 214 (2002) 383–395) © 2002 Elsevier Science B.V. All rights reserved.

Keywords: FT/ICR-MS; Gallium cluster; Jellium model; LDI

1. Introduction

In the last decades "naked" clusters of metal atoms have provided a fascinating object for experimental and theoretical studies due to their particular chemical and physical properties [1,2]. Stabilization of the normally very reactive clusters can be achieved by the protective sphere of ligands. The clusters then consist of a metal core shielded by organic ligands [3]. This type of structurally characterized clusters exists for a number of precious metals [4–6]. However, we established a method that allows the preparation of large aluminum and gallium clusters (e.g., $Al_{77}R_{20}^{2-}$, $Ga_{84}R_{20}^{4-}$, $Al_{69}R_{18}^{3-}$ [7–9]) which are—with respect to the number of non-ligand-bearing metal atoms—the largest metalloid clusters ever characterized by means of X-ray diffraction analysis.

Gallium clusters of this type are prepared starting from a gallium(I) halide solution, which is obtained after condensation of organic solvents together with gaseous GaBr (at −196 °C) generated in a gas–liquid reaction from hydrogen halide and gallium at 800 °C. Upon heating to room temperature, the metastable solution disproportionates to give elemental gallium and trivalent gallium compounds. By the use of suitable

* Corresponding author.
E-mail: hansgeorg.schnoeckel@chemie.uni-karlsruhe.de

1387-3806/02/$20.00
PII S1387-3806(02)00543-2

stabilizing ligands (e.g., $CSi(CH_3)_3$) intermediates of this process, that is gallium clusters, can be trapped and characterized by means of X-ray diffraction analysis [3,10,11].

The formation mechanism and the fragmentation pattern of these clusters are in the center of interest in our investigations, since they provide information about the mechanism of one of the oldest chemical processes of mankind: the formation of metals starting from ore, and their oxidation giving saline solutions. Other groups and our group have studied some steps of this reaction in solution and obtained metalloid gallium clusters containing 6–84 gallium atoms [12]. In order to improve the knowledge of the formation/dissolution mechanism of metalloid clusters, we have started with some gas phase investigations by means of FT/ICR-MS.

To the best of our knowledge, the metalloid cluster $[Ga_{19}(C(SiMe_3)_3)_6][Li_2Br(THF)_6]$ **1** is the first molecular cluster compound which releases naked clusters after laser desorption. Like the metalloid clusters in solution, the "naked" clusters in the gas phase might represent intermediates on the way to the bulk metal. Since laser desorption is a very "crude" method for ionization and vaporization of such labile compounds some naked silicon-doped gallium clusters are generated in addition, which are to our knowledge firstly investigated in this paper.

The high abundance of certain gallium and silicon-doped gallium clusters in our mass spectrum can partly be rationalized from the molecular structure of **1** and is different from all experiments described before which started from solid or liquid gallium or gallium alloys [13–15]. Moreover, there exist only a few publications on mass spectra of gallium and by far not as many as for the lighter homologue aluminum [16–18]. Theoretical investigations on gallium clusters mostly focus on the neutral clusters [19,20].

Our experiments were accompanied by quantum chemical calculations of the Ga_{13}^- and the $Ga_{12}Si^-$ anion. To our knowledge this is the first quantum chemical study of such a big anionic gallium cluster and a mixed gallium–silicon cluster. The results of our calculations were compared with the predictions of the jellium model. [1]

Density functional theory (DFT) has proved to be a suitable method for the calculation of gallium cluster [20] species and therefore, this method was used throughout this work. The results are compared with those obtained for the neutral cluster presented in a previous theoretical study [19].

2. Experimental

Experiments were carried out using a GSG/IonSpec HiresMALDI (Bruchsal, Germany and Irvine, CA) Fourier-transform ion cyclotron resonance (FT/ICR) mass spectrometer, equipped with a 5.2 cm long cylindric trapping cell situated in the bore of a 7 T superconducting magnet (Cryomagnetics Inc., Oak Ridge, Tennessee). Two cryo pumps and a turbo molecular pump maintain a base-pressure of 1×10^{-10} Torr in the cell region. To generate pure metal cluster ions, we used an external laser desorption ionization (LDI) source, equipped with a pulsed N_2-laser ($\lambda = 337.1$ nm). The storage time of the cluster ions in the ICR-cell varied between 6 and 30 s.

The species $[Ga_{19}(C(SiMe_3)_3)_6][Li_2Br(THF)_6]$ **1**, which we used in the present study, was prepared by adding $LiC(SiMe_3)_3$ to a metastable GaBr solution in toluene/THF at $-78\,^{\circ}C$ [3].

All calculations were carried out with the DFT implementation of TURBOMOLE [21] using the Becke-Perdew-86 (BP-86) functional [22,23]. Coulomb interactions were treated within the resolution of the identity (RI) approximation [24]. The grids required

[1] The shell or jellium model explains the striking stability of special metal clusters by means of their electronic structure [33]. In this model, one assumes that the clusters are spherical and the charge is dispersed uniformly over the whole cluster. One ends up with free electrons in a spherical potential. The simplest form for such a potential is the harmonic oscillator with a highly degenerated shell structure of spherical harmonics (1s) (1p) (2s, 1d) (2p, 1f) (3s, 2d, 1g) .... This means, that clusters with "magic" electron numbers $n_{el} = 2, 8, 20, 40, 70, \ldots$ should be exceedingly stable ("magic" in cluster studies generally refers to a number of electrons, atoms etc., belonging to an exceptionally stable cluster).

for the numerical integration of the exchange and correlation contributions were of medium coarseness [25]. The basis set was of split valence plus polarization (SVP) type [26]. Nuclear magnetic resonance (NMR) shifts were calculated using the gauge including atomic orbital (GIAO) method [27]. Data of $Ga(C_5H_5)$ were used as reference [28].

3. Results

Fig. 1 shows a typical mass spectrum of the anions ejected from **1** by LDI. It is composed of several spectra of different measurements and ranges from 200 up to 4000 amu. The spectrum indicates the presence of several pure gallium clusters Ga_n^- with $n = 4$–50 which can be deduced from the exact mass measurements and the isotopic distribution. Additional signals of much lower intensity within this spectrum can be associated with silicon-doped gallium clusters of the general formula $Ga_nSi_m^-$ ($n = 5$–43; $m = 1$–3).

Fig. 2 shows the same mass spectrum with the component mass spectra of Ga_n^- homologous series and the Ga_nSi^- homologous series separated from one another in Fig. 2a and b, respectively. The intensities of the strongest peak in each spectrum are normalized to the same value for better comparison. A maximum of the cluster abundance in Fig. 2a is observed for Ga_{13}^-. Its signal is in average 10 times more intense than the signal of the next intense Ga_{23}^- cluster. Furthermore, it can be seen that clusters with an odd number n of gallium atoms are in general significantly larger in intensity compared to those with a neighboring even number $n \pm 1$. Since the clusters are negatively charged an odd number of gallium atoms implies always an even number of electrons.

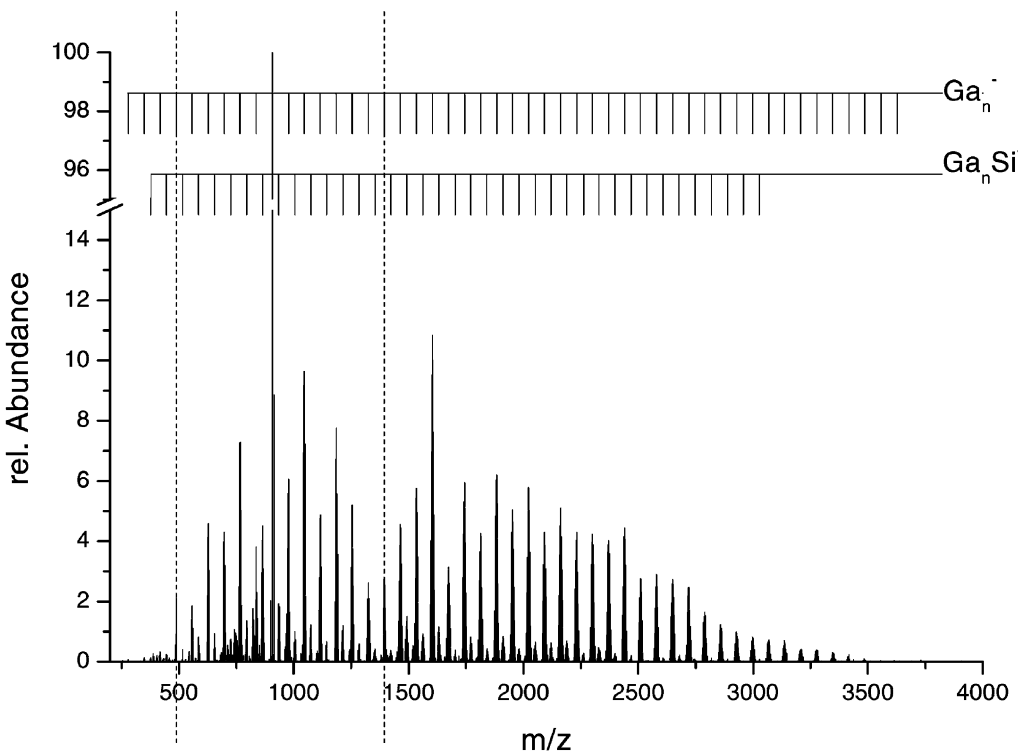

Fig. 1. Typical FT/ICR mass spectrum of **1**, negative ions, produced during laser desorption ionization, resolving power ≈ 170,000 (related to the signal at 906 amu), mass accuracy = 2 ppm. (The spectrum is composed of several single spectra, indicated with a dashed line.)

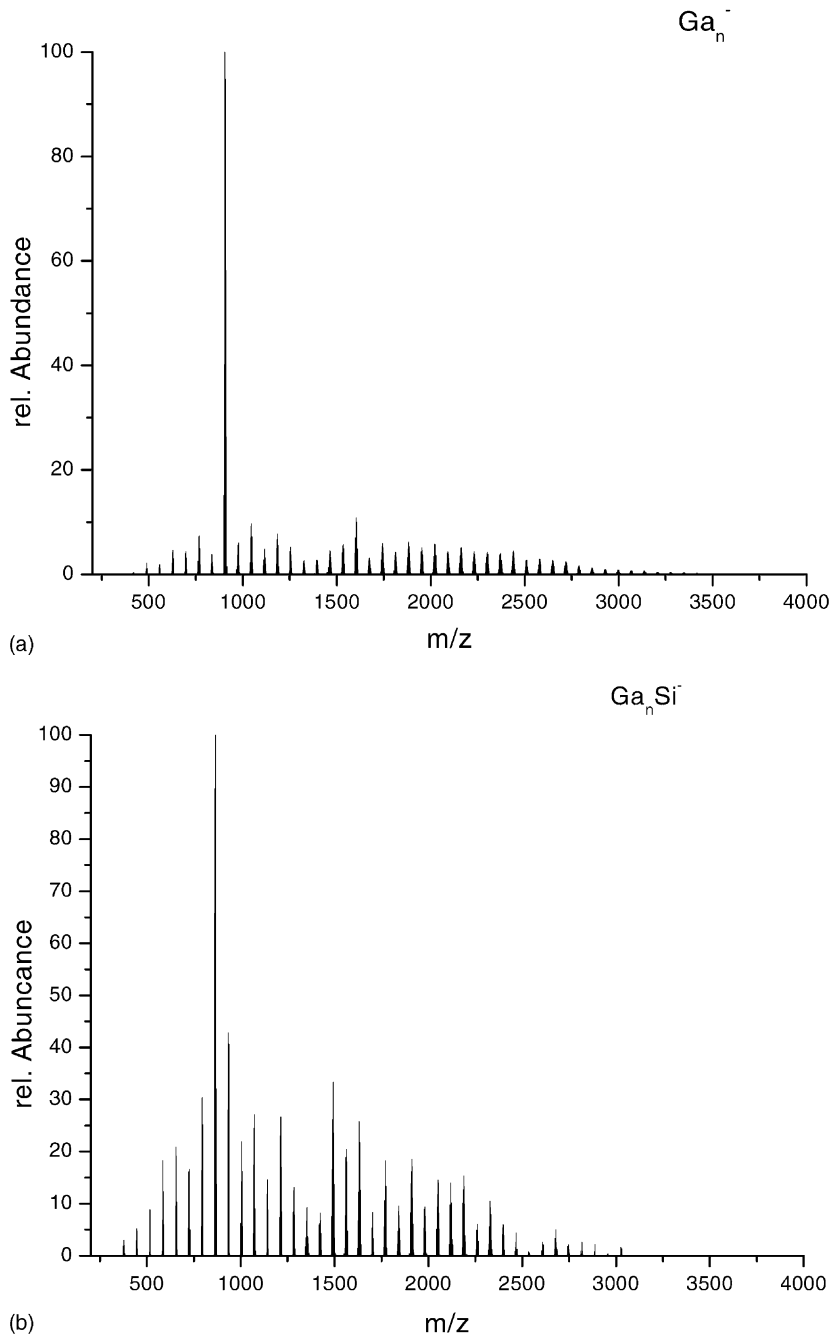

Fig. 2. This is the same mass spectrum as in Fig. 1 but with the component mass spectra of the Ga_n^- homologous series and the Ga_nSi^- homologous series separated from one another in (a) and (b), respectively. The intensities of the strongest signal in each spectrum have been normalized to the same value, i.e. (b) has been magnified by a factor of 22.

The mass spectrum in Fig. 2b is dominated by $Ga_{12}Si^-$. Its signal is more than 20 times less intense than the signal of the Ga_{13}^- cluster, the cluster of the highest abundance in the Ga_n^- homologous series. The ratio of the intensities of a Ga_n^- cluster and its corresponding Ga_nSi^- cluster varies between approximately 50:1 (Ga_{13}^- to $Ga_{13}Si^-$) and 1:1.2 (Ga_{12}^- to $Ga_{12}Si^-$). But generally, the intensity of the Ga_nSi^- cluster is less intense than the corresponding Ga_n^- cluster. The $Ga_nSi_m^-$ ($m = 2, 3$) species are also present in the spectrum, but they are only discernible at very low ion intensities. Ga_4^- is the smallest observable anionic gallium cluster. In contrast, the spectrum of the cations does not reveal any gallium clusters, but only exhibit signals which can be assigned to both gallium isotopes $^{69}Ga^+$ and $^{71}Ga^+$, the ligand cation $C(SiMe_3)_3^+$ and its secondary dissociation product $SiMe_3^+$ (see Fig. 3). Remaining signals of lower intensity within this spectrum refer to impurities and cannot be specified more precisely.

The signals in the spectrum were identified via exact mass measurement and the comparison with the theoretical isotopic pattern. In Fig. 4, the spectra obtained for Ga_{13}^- and Ga_{23}^- are presented together with the corresponding theoretically calculated isotopic distributions. Generally, variations in the intensity of the laser with the aid of an aperture as well as in the storage time of the ions in the ICR-cell do not change the characteristic appearance of the spectrum. That means, that the relative intensities of the ions remain the same.

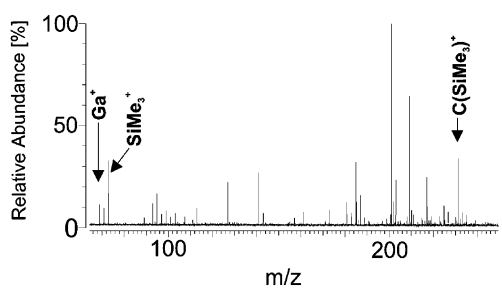

Fig. 3. FT/ICR mass spectrum of **1**, positive ions.

4. Discussion

4.1. Ga_n^- cluster anions

The most intense signal in the spectrum belongs to the Ga_{13}^- cluster, its intensity being more than 10 times as high as the next intense signal in the spectrum. In general, this is expected, since Ga_{13}^- is a 40 electron cluster and thus, possesses a closed shell structure (see footnote 1). It is expected to be quite stable and in fact, it is the result of numerous magic number cluster studies that such clusters represent a peak in the mass spectrum of "naked" clusters [16,29]. However, the signal for Ga_{13}^- in the spectrum presented in this paper, is not only twice or three times as intense as the next intense signal, it is more than 10 times as intense as the signal for Ga_{23}^- and even 15 and 25 times more intense than the two gallium clusters nearest in mass (Ga_{14}^- and Ga_{12}^-). This large difference in intensity can hardly be explained on the basis of the simple jellium model, since Ga_{23}^- also possesses a closed shell structure.

Insight on the cluster distribution is gained after a look at the structure of the precursor. **1** has been structurally characterized previously by means of X-ray diffraction analysis [3]. It consists of 1 central gallium atom surrounded by 12 non-ligand-bearing gallium atoms. The geometric arrangement of these atoms is between anticuboctahedral and icosahedral. The remaining six gallium atoms each carry one ligand and are bonded to three non-ligand-bearing atoms of the Ga_{13}^- core (see Fig. 5e).

Thus, one reason for the high intensity of the Ga_{13}^- signal in the mass spectrum is presumably due to its formation mechanism during LDI:

$$Ga_{13}(GaR)_6^- \rightarrow Ga_{13}^- + GaR$$

This hypothetic decomposition route appears reasonable since the remaining cluster contains just those 13 gallium atoms which are not ligand-bearing. Furthermore, the existence of neutral GaR units is observed to be thermodynamically stable at low pressure and high temperatures (see: GaCl, GaBr, $Ga(C_5Me_5)$ etc. [30,31]). Moreover, recent calculations on the

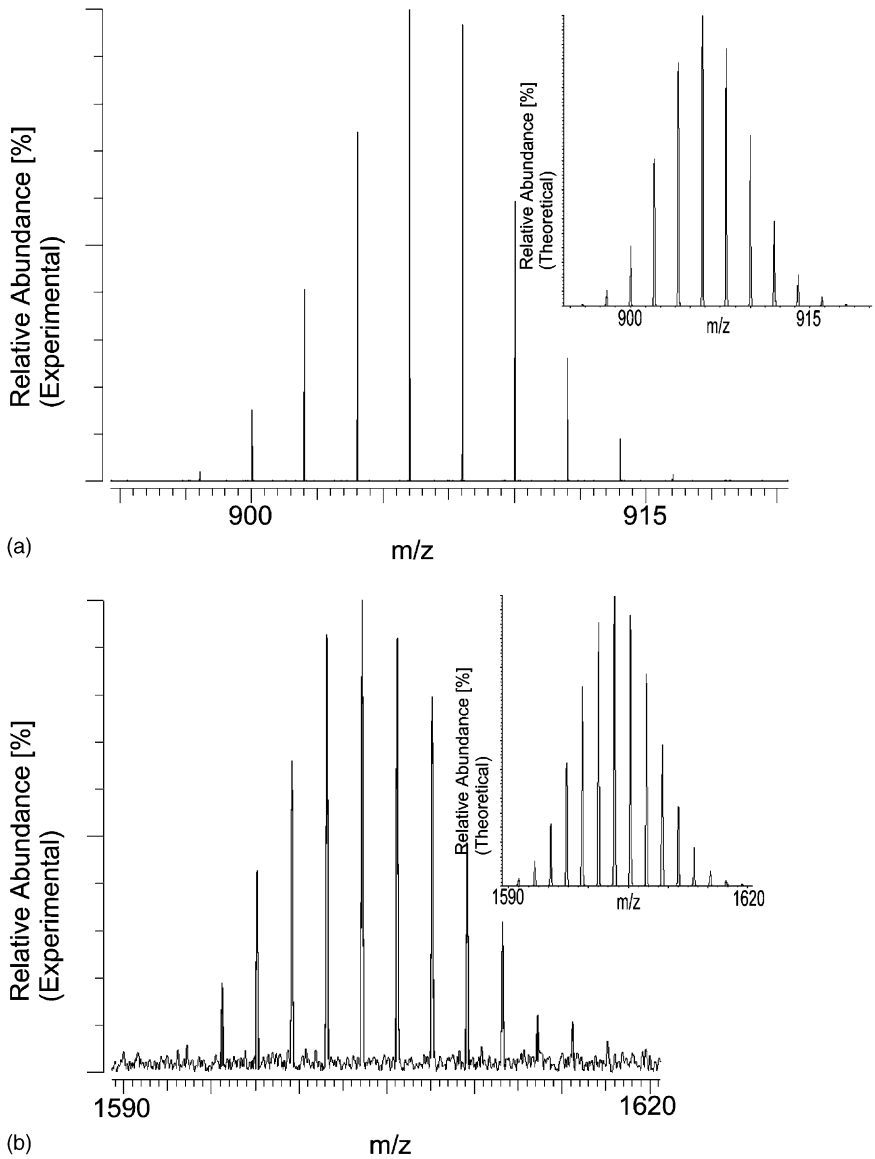

Fig. 4. FT/ICR mass spectra of the Ga_{13}^- cluster (a) and the Ga_{23}^- cluster (b) and the corresponding calculated spectra.

metalloid cluster $Al_{77}R_{20}^{2-}$ ($R = N(SiMe_3)^2$) of the lighter homologue aluminum have shown, that this cluster cannot be described as a Al_{77}^{18+} cluster which would result after removal of 20 ligands. But the cluster can best be understood as a Al_{57}^{2-} cluster one obtains after removal of 20 neutral AlR unities [32] (Fig. 6).

Another reason for the high intensity of the Ga_{13}^- anion in the spectrum is its electronic structure as mentioned above, which is in accordance with the shell or jellium model [33,34], since the electron number of the Ga_{13}^- anion is $13 \times 3 + 1 = 40$. Thus, to gain an insight into the structure of Ga_{13}^-, we performed DFT calculations.

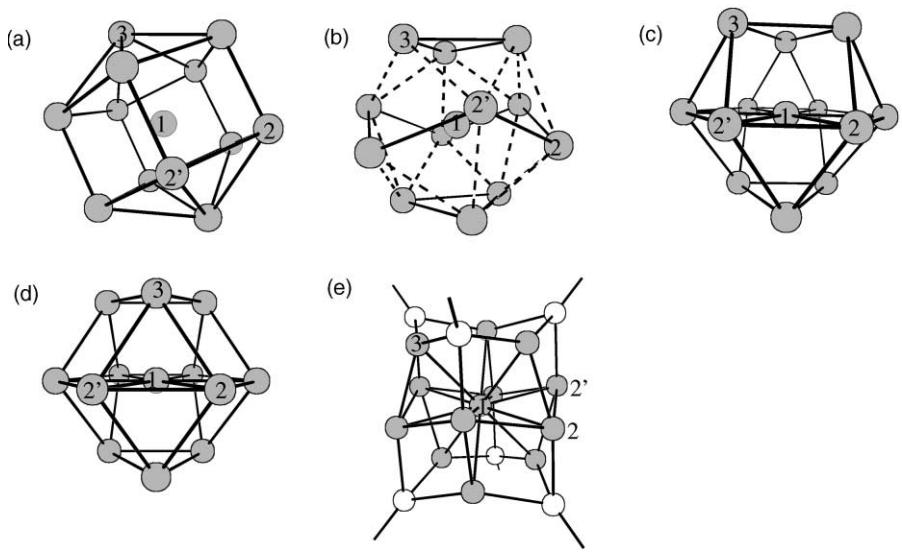

Fig. 5. Calculated structures of (a) the bicapped pentagonal prismatic, (b) the icosahedral, (c) the cuboctahedral, (d) the anticuboctahedral Ga_{13}^- cluster, and (e) the structure of **1** as derived from the experimental data.

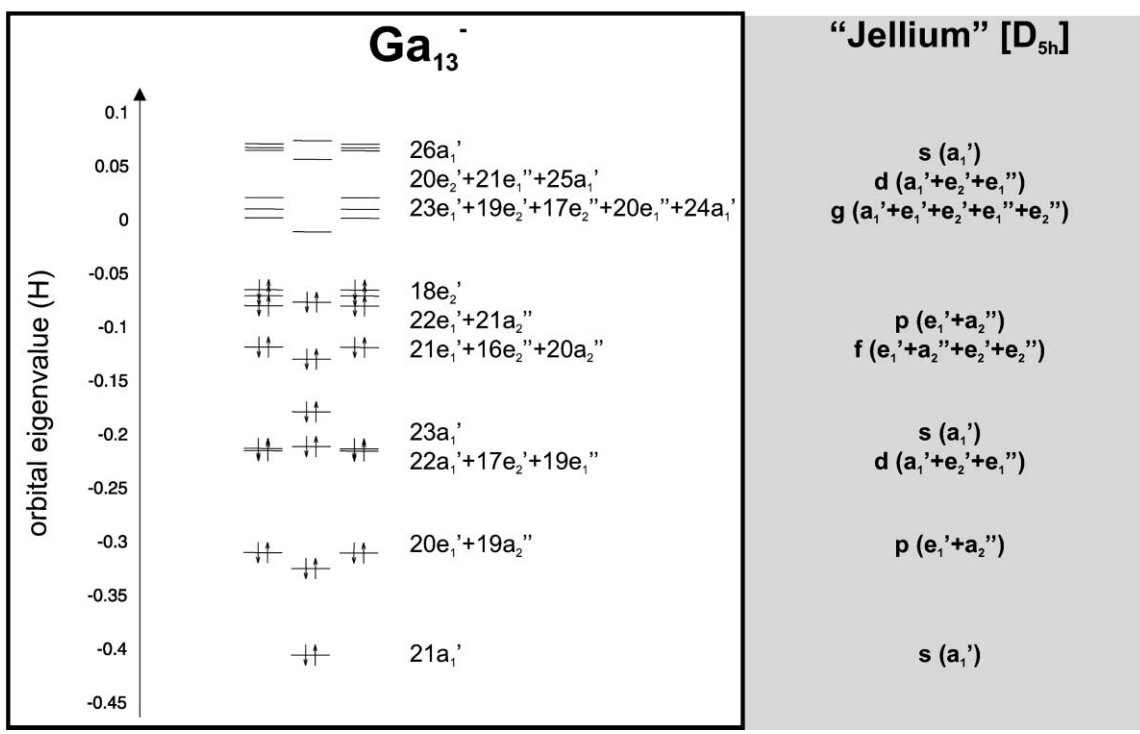

Fig. 6. MOs of the Ga_{13}^- bicapped pentagonal prism (D_{5h}) and the expected MO separation concluded from the jellium model.

Table 1
Calculated geometries (in Å), ^{71}Ga NMR shifts and relative stability (ΔE in eV) of the bicapped pentagonal prismatic, the icosahedral, the cuboctahedral, the anticuboctahedral Ga_{13}^- clusters, and the experimentally obtained data for **1** [3]

Ga_{13}^- unit	Symmetry	ΔE	Dist 1–2	Dist 1–3	Dist 2–2′	δ^{71}Ga (central)	Figure
Bicapped pentagonal prism	D_{5h}	–	2.754	2.703	2.863	510.5	(5a)
Icosahedron	I_h	0.350	2.696	2.696	2.835	622.0	(5b)
Cuboctahedron	O_h	1.259	2.747	2.747	2.747	644.8	(5c)
Anticuboctahedron	D_{3h}	0.224	2.746	2.757	2.589	502.1	(5d)
1 (experimental)	–	–	2.837	2.959	2.896	134	(5e)

Table 2
Calculated geometries (in Å), ^{71}Ga NMR shifts and electron affinities (vertical detachment energies and adiabatic electron affinities in eV) of the distorted bicapped pentagonal prismatic, the distorted icosahedral and the distorted cuboctahedral neutral Ga_{13} cluster

Ga_{13}^- unit	Symmetry	ΔE[a]	Dist 1–2	Dist 1–3	Dist 2–2′	δ^{71}Ga (central)	EA
Distorted bicapped pentagonal prism	C_{2v}	–	2.7385 (av)	2.746	2.860 (av)	−454.6	−3.59
Distorted icosahedron	C_3	0.368	2.742	2.697	2.939	−577.8	−3.59
Distorted cuboctahedron	D_{3d}	0.894	2.751	2.768	2.751	−620.8	−3.03

[a] ΔE (in eV) is the relative energy to the ground state.

The geometry of the "naked" anionic Ga_{13}^- cluster in its ground state is not anticuboctahedral nor icosahedral nor cuboctahedral but a bicapped pentagonal prism (Table 1). The distances Ga1–Ga2 and Ga1–Ga3 are 2.7545 and 2.703 Å, respectively (in comparison to 2.837 and 2.959 Å in the crystallographically determined Ga_{13}^- subunit of **1**, Table 1). The total energy of this bicapped pentagonal prism (D_{5h}) is smaller than that of the icosahedron, the cuboctahedron and the anticuboctahedron by 0.350, 1.259 and 0.224 eV. Neither the icosahedron nor the cuboctahedron nor the anticuboctahedron were found to be minima on the potential energy hypersurface, but saddle points. The same result is found for some distorted structures investigated but not listed in Table 1. The bicapped pentagonal prism is the only true minimum found (Fig. 5).

The structures calculated herein for the neutral Ga_{13} species are in pleasing agreement to the results of Yi [19]. We also find a (Jahn-Teller-distorted) bicapped pentagonal prism with a total energy smaller than that of the relaxed icosahedron and cuboctahedron by 0.58 and 0.89 eV, respectively (0.22 and 0.67 eV, respectively, found by Yi [19]). But as in the anionic species, here as well, our calculations show, that only the (distorted) bicapped pentagonal prism is a minimum on the potential energy hypersurface (see Table 2).

The electron affinity (vertical detachment energy) is calculated to be 3.59 eV for both the bicapped pentagonal prismatic (D_{5h}) and the icosahedral structure of Ga_{13}. The adiabatic electron affinity is 3.35 eV for the bicapped pentagonal prismatic (D_{5h}) and 3.37 eV for the icosahedral structure, respectively. This compares with values of 3.60 and 3.57 eV obtained by Yi [19]. It is worth mentioning, that in the gallium bulk bicapped pentagonal prismatic structures are not known.

By a closer look on the sequence of the DFT molecular orbitals, the congruence between the electronic structure of the Ga_{13}^- anion (D_{5h}) as derived from our DFT studies and the expected molecular orbital separation according to the jellium model is confirmed [2].

[2] Besides these investigations of the ground state geometries and energies directly relevant for this work, the ^{71}Ga NMR shift of the central gallium atom have been calculated. For the central atom in the "naked" neutral and anionic Ga_{13} species (distorted decahedral and decahedral species, respectively) δ^{71}Ga is calculated to be −455 and −511 ppm, respectively (see Tables 1 and 2). This value can be compared with the experimentally detected ^{71}Ga NMR shift for **1**, it is detected at $\delta^{71}\text{Ga} = -134$ ppm for the central Ga atom [3]. The differences between the structural parameters measured in **1** and calculated in the naked Ga_{13} species as well as the large differences in the ^{71}Ga NMR shifts of the central gallium show, that it is difficult to decide, which type of cluster—naked or ligand stabilized—would constitute a better model compound for the bulk metal.

But the extremely high abundance of the Ga_{13}^- cluster cannot solely be explained on the basis of the jellium model. However, it is a suitable model to explain the relative abundances of the other clusters found in the spectrum, because they are presumably products of secondary gas phase reactions. For example, the second intense signal in the mass spectrum belongs to the Ga_{23}^- cluster. With an electron number of $(3 \times 23 + 1 = 70)$ it also exhibits a closed shell jellium structure. Besides this, it is a general feature of the spectrum, that signals due to clusters with an even number of electrons are more intense than those belonging to clusters with an odd number of electrons.

4.2. Ga_nSi^- cluster anions

The formation mechanism of these clusters appears to be considerably complicated, e.g., the mass spectrum of the Ga_nSi^- series is dominated by $Ga_{12}Si^-$. This cannot be explained with the help of the precursor's structure, because it does not feature any gallium–silicon bonds. Thus, the $Ga_{12}Si^-$ cluster was generated inside the plume that forms during the laser shot. Its abundance with respect to the other Ga_nSi^- clusters cannot be explained with the help of the simple jellium model. $Ga_{12}Si^-$ is a 41 electron cluster, that is one electron more than the number needed to form a closed electronic shell. Clusters of this type are normally very unstable. Bowen and co-workers [16] recently published a mass spectrum of Al_nCu^- clusters, also showing an intensity maximum for the 41 electron cluster $Al_{13}Cu^-$. The authors explain the unusual number of the 41 electron $Al_{13}Cu^-$ cluster by a jellium-like potential shape with a depression in the center of the cluster. This depression is a result of the high positive charge density of copper [35]. This causes a rearrangement of the spherical electronic shell levels. The new ordering of electronic shell levels is (1s), (1p), (2s, 1d), (1f, 2p), (3s, 1g, 2d), ... in contrast to (1s), (1p), (1d, 2s), (1f, 2p), (1g, 2d, 3s), ... of a "normal" jellium cluster. Thus, 42 becomes a new magic number. As a consequence $Al_{13}Cu^-$ has one electron less than is needed to fill a closed shell. This often exhibits a local intensity maximum in the mass spectrum.

In order to use this explanation with our $Ga_{12}Si^-$ cluster, we first investigated its doublet ground state (Fig. 7). The ground state structure of $Ga_{12}Si^-$ is not

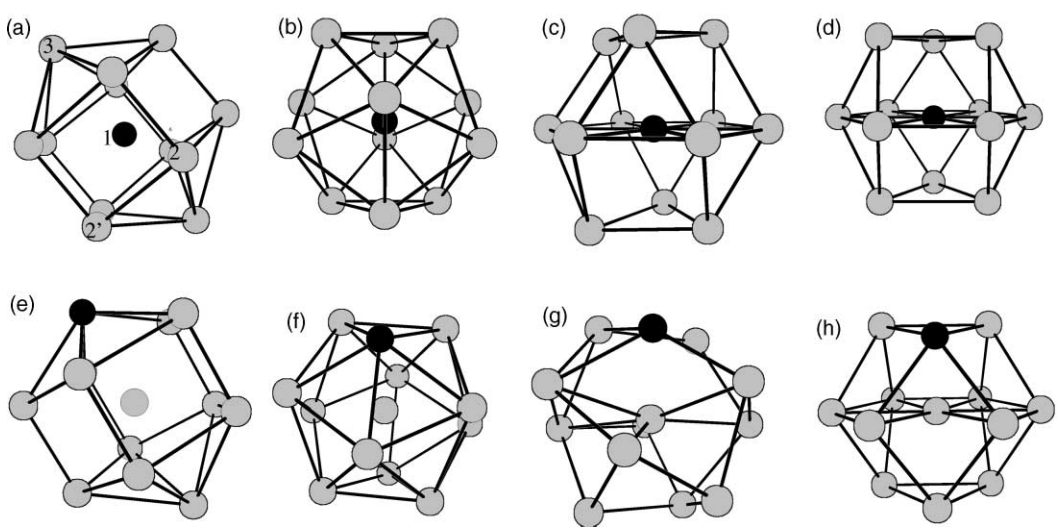

Fig. 7. Calculated structures of (a) the bicapped pentagonal prismatic, (b) the icosahedral, (c) the cuboctahedral, (d) the anticuboctahedral $Ga_{12}Si^-$ cluster (silicon in the center); (e) the bicapped pentagonal prismatic, (f) the icosahedral, (g) the cuboctahedral, (h) the anticuboctahedral $Ga_{12}Si^-$ cluster (silicon in the external shell).

Table 3
Relative stability (ΔE in eV) of the distorted bicapped pentagonal prismatic, the distorted icosahedral, the distorted cuboctahedral, and the distorted anticuboctahedral $Ga_{12}Si^-$ cluster

$Ga_{12}Si^-$ unit	Silicon in the center			Silicon in the external shell		
	Symmetry	ΔE	Figure	Symmetry	ΔE	Figure
Bicapped pentagonal prism	D_{5h}	–	(7a)	C_{5v}	0.626	(7e)
Distorted icosahedron	D_{5d}	0.457	(7b)	C_{5v}	0.849	(7f)
Distorted cuboctahedron	D_{4h}	1.521	(7c)	C_s	0.651	(7g)
Distorted anticuboctahedron	C_{2v}	0.302	(7d)	C_s	0.830	(7h)

Table 4
Relative stability (ΔE in eV) and adiabatic electron affinity of the bicapped pentagonal prismatic, the icosahedral, the cuboctahedral, and the anticuboctahedral neutral $Ga_{12}Si$ cluster

$Ga_{12}Si^-$ unit	Silicon in the center			Silicon in the external core		
	Symmetry	ΔE	EA	Symmetry	ΔE	EA
Bicapped pentagonal prism	D_{5h}	–	2.21	C_{5v}	0.823	2.41
Icosahedron	I_h	0.362	2.12	C_{5v}	0.953	2.31
Cuboctahedron	O_h	1.363	3.02	C_{2v}	1.177	2.74
Anticuboctahedron	D_{3j}	0.252	2.16	C_s	0.922	2.30

anticuboctahedral nor icosahedral nor cuboctahedral but a bicapped pentagonal prism (Table 3), the silicon atom being located in the center of the polyhedron. The distances Si–Ga2 and Si–Ga3 are 2.716 and 2.934 Å, respectively. The total energy of this $Ga_{12}Si^-$ D_{5h} cluster is smaller than that of the icosahedron, the cuboctahedron and the anticuboctahedron by 0.46, 0.56 and 0.30 eV, respectively. If the silicon atom is situated in the external gallium core the total energy is higher in every geometrical arrangement. By frequency calculations the silicon-centered D_{5h} ground state is confirmed to be the only true minimum of all conceivable structures. The adiabatic electron affinity of this silicon-centered D_{5h} cluster is calculated to be 2.21 eV (Table 4).

A closer look on the sequence of the DFT molecular orbitals of $Ga_{12}Si^-$ (D_{5h}) does partly confirm the explanation of Bowen and co-workers [16] and Khanna et al. [35], respectively, for the unusual magic number of 41 electrons. The 2s shell of the $Ga_{12}Si^-$ cluster is in fact much lower in energy than in the $Ga_{13}{}^-$ cluster with respect to the 1d shell (see Fig. 8). Whether or not the 3s shell has drop in between the 2p and 1g shell is difficult to decide, since both, 3s and 1g exhibit orbitals of a_1' symmetry. This congruency between the $Al_{13}Cu^-$ cluster of Bowen and co-workers [16] and the $Ga_{12}Si^-$ cluster is evident, since the ionization energies of silicon and gallium compare with those of copper and aluminum. It is 8.1 eV for silicon (7.7 eV for copper) and 6 eV for both, gallium and aluminum, respectively.

A comparable electronic situation to that of $Ga_{12}Si^-$ is found in $SiAl_{14}Cp^*_6$, which was the first example that accounts for the validity of the jellium model if only species are considered that are stable at room temperature [36]. The structure of this compound was investigated both by X-ray diffraction methods and by theoretical density functional theory. The $SiAl_{14}{}^{6+}$ metal cluster core contains 40 electrons, silicon resides in the center of an Al_8 cube. In Fig. 9, the valence MOs of the model compound $SiAl_{14}H_6$ and the expected MO separation concluded from the jellium model are presented.[3] The energy of the molecular orbital 10 a_{1g} is lower than that of the molecular orbitals $6t_{2g}$ and $5e_g$ that are attributed

[3] Due to an editorial error in the original paper [36], this figure is presented again here.

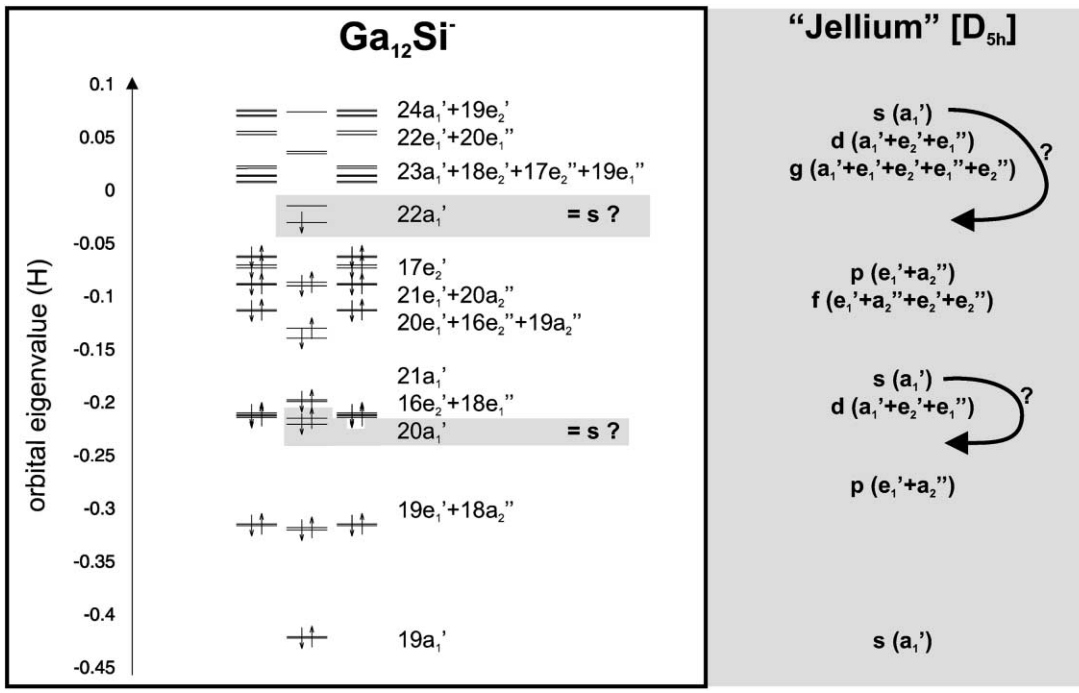

Fig. 8. Spin orbitals of the $Ga_{12}Si^{-}$ bicapped pentagonal prism (D_{5h}), compared with the MO separation concluded from the jellium model.

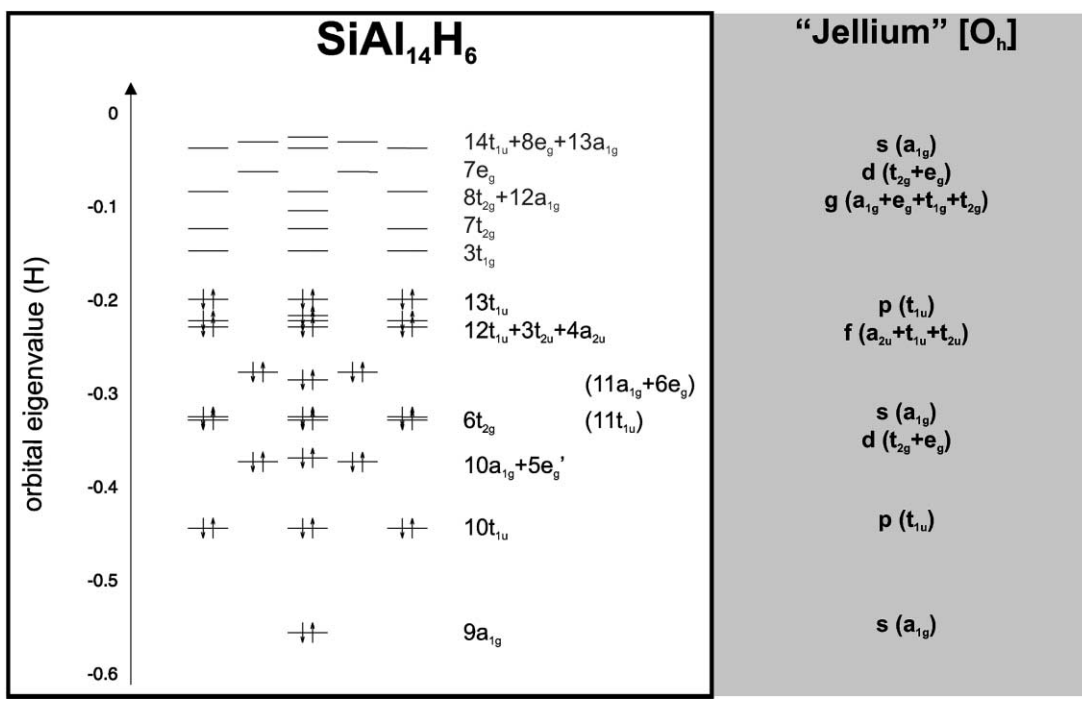

Fig. 9. MOs of $SiAl_{14}H6$ (O_h), compared with the MO separation for an octahedral structure concluded from the jellium model.

to the 2s and 1d jellium shells, respectively. Silicon plays a similar role in both compounds. The silicon atom holds a highly negative atomic charge of −0.99 [37] in $SiAl_{14}Cp^*_6$ and −0.91 in $SiGa_{12}$. Although gallium, silicon and aluminum have similar atomic radii a discussion of bond distances is not helpful due to the varying coordination spheres in these molecules and ions.

The MO sequence of Ga_{13}^- and $Ga_{12}Si^-$ do not differ too much from one another. Furthermore, one has to keep in mind, that a rearrangement of the shell orbitals does perhaps generate new subshells, but the main shells still remain more or less the same. To sum up, in our opinion this modified jellium model is only the first attempt in order to explain the abundance of the $Ga_{12}Si^-$ cluster in our spectrum. On the other hand, we are so far not able to offer a better explanation for the intense appearance of the $Ga_{12}Si^-$ cluster.

5. Summary and conclusion

Herein we have shown that the mass spectrum of a ligand-stabilized metalloid gallium cluster reveals "naked" metal cluster ions when used as target for laser desorption, namely the gallium clusters Ga_n^- ($n = 4$–50). Additionally, the mixed gallium–silicon clusters $Ga_nSi_m^-$ ($n = 5$–43; $m = 1$–3) are formed as a result of the presence of silicon in the ligand-sphere of the cluster.

The particular abundance of the Ga_{13}^- cluster in the spectrum is best interpreted with the help of the formation mechanism of this cluster. It is directly formed starting from the precursor and gives a hint on the formation mechanism and degradation of this kind of clusters as intermediates on the way from covalent gallium compounds to bulky gallium metal.

The dominant cluster of the Ga_nSi^- series in the spectrum is $Ga_{12}Si^-$. In contrast to Ga_{13}^-, this cluster as well as all other clusters in the spectrum are likely to be formed in secondary gas phase reactions. Thus, their abundance pattern is compared with the predictions of the theoretically deduced jellium model. For this purpose, theoretical calculations are employed. Both, the $Ga_{12}Si^-$ and the Ga_{13}^- cluster possess a bicapped pentagonal prismatic ground state structure. While the Ga_{13}^- cluster indeed is a closed shell cluster, we are at the moment not in the position to give a satisfying explanation for the abundance of $Ga_{12}Si^-$ in the Ga_nSi^- component spectrum. Nevertheless, our theoretical results verify and complete recently published studies.

Additional measurements of the ionization potentials are on the way in order to confirm the theoretical results. Furthermore, gas phase reactions of the "naked" clusters are planned by means of FT/ICR-MS in order to understand the chemical reactivity of "naked" gallium clusters. However, the most important experiments in the future will focus on details of the formation and decomposition mechanism of **1**.

References

[1] E. Schmid (Ed.), Cluster and Colloids, VCH, Weinheim, 1994.
[2] P. Braunstein, L.A. Oro, P.R. Raithby, Metal Clusters in Chemistry, Wiley, Weinheim, 1999.
[3] A. Schnepf, G. Stösser, H. Schnöckel, J. Am. Chem. Soc. 122 (2000) 9178.
[4] N.T. Tran, M. Kawano, D.R. Powell, L.F. Dahl, J. Am. Chem. Soc. 120 (1998) 10986.
[5] N.T. Tran, D.R. Powell, L.F. Dahl, Angew. Chem. 112 (2000) 4287;
N.T. Tran, D.R. Powell, L.F. Dahl, Angew. Chem. Int. Ed. Engl. 39 (2000) 4121.
[6] B.K. Teo, X. Shi, H. Zhang, J. Am. Chem. Soc. 114 (1992) 2743.
[7] A. Schnepf, H. Schnöckel, Angew. Chem. 113 (2001) 737;
A. Schnepf, H. Schnöckel, Angew. Chem. Int. Ed. Engl. 40 (2001) 711.
[8] A. Ecker, E. Weckert, H. Schnöckel, Nature 387 (1997) 379.
[9] H. Köhnlein, A. Purath, C. Klemp, E. Baum, I. Krossing, G. Stößer, H. Schnöckel, Inorg. Chem. 40 (2001) 4830.
[10] C. Dohmeier, D. Loos, H. Schnöckel, Angew. Chem. 108 (1996) 141.
[11] A. Donchev, A. Schnepf, G. Stößer, E. Baum, H. Schnöckel, T. Blank, N. Wiberg, Chem. Eur. J. 7 (2001) 3348.
[12] H. Schnöckel, A. Schnepf, Advanc. Organmetallic Chem. 47 (2001) 235.
[13] C. Cha, G. Ganteför, W. Eberhardt, Ber. Bunsenges. Phys. Chem. 96 (1992) 1223.
[14] F.L. King, B.I. Dunlap, D.C. Parent, J. Chem. Phys. 94 (1991) 2578.
[15] Y. Saito, K. Mihama, T. Noda, in: T. Arai, K. Mihama, K. Yamamoto, S. Sugano (Eds.), Mesoscopic Materials and Clusters: Their Physical and Chemical Properties, Springer, Berlin, 1999, p. 321.

[16] O.C. Thomas, W. Zheng, K.H. Bowen Jr., J. Chem. Phys. 114 (2001) 5514.
[17] R.E. Leuchtner, A.C. Harms, A.W. Castleman Jr., J. Chem. Phys. 91 (1989) 2753.
[18] B.D. Leskiw, A.W. Castleman Jr., C. Ashman, S.N. Khanna, J. Chem. Phys. 114 (2001) 1165.
[19] J.-Y. Yi, Phys. Rev. B 61 (2000) 7277.
[20] R.O. Jones, J. Chem. Phys. 99 (1993) 1194.
[21] O. Treutler, R. Ahlrichs, J. Chem. Phys. 102 (1995) 346.
[22] J.P. Perdew, Phys. Rev. B 33 (1986) 8822.
[23] A.D. Becke, Phys. Rev. A 38 (1988) 3098.
[24] K. Eichkorn, O. Treutler, H. Öhm, M. Häser, R. Ahlrichs, Chem. Phys. Lett. 240 (1995) 283.
[25] K. Eichkorn, F. Weigend, O. Treutler, R. Ahlrichs, Theor. Chem. Acc. 97 (1997) 119.
[26] A. Schäfer, H. Horn, R. Ahlrichs, J. Chem. Phys. 97 (1992) 2571.
[27] G. Schreckenbach, T. Ziegler, J. Phys. Chem. 99 (1995) 606.
[28] D. Loos, H. Schnöckel, J. Gauss, K. Schneider, Angew. Chem. 104 (1992) 1976.
[29] W.D. Knight, K. Clemenger, W.A. De Heer, W.A. Saunders, M.Y. Chou, M.L. Cohen, Phys. Rev. Lett. 52 (1984) 2141.
[30] A. Haaland, K.-G. Martinsen, H.V. Volden, D. Loos, H. Schnöckel, Acta Chem. Scand. 48 (1994) 172.
[31] M.W. Chase, JANAF Thermochemical Tables, Vol. 14, American Institute of Physics, New York.
[32] X.G. Gong, D.Y. Sun, X.-Q. Wang, Phys. Rev. B 62 (2000) 15413.
[33] W.A. de Heer, W.D. Knight, M.Y. Chou, M.L. Cohen, Solid State Phys. 40 (1987) 93.
[34] A. Köhn, F. Weigend, R. Ahlrichs, Phys. Chem. Chem. Phys. 3 (2001) 711.
[35] S.N. Khanna, C. Ashman, B.K. Rao, P. Jena, J. Chem. Phys. 114 (2000) 9792.
[36] A. Purath, C. Dohmeier, A. Ecker, R. Köppe, H. Krautscheid, H. Schnöckel, R. Ahlrichs, C. Stoermer, J. Friedrich, P. Jutzi, J. Am. Chem. Soc. 122 (2000) 6955.
[37] R. Köppe, private communication.